16th World Conference on Earthquake Engineering, 16WCEE 2017
Santiago Chile, January 9th to 13th 2017
Paper N° 2037
Registration Code: S-I14654524744

Influence of Axial Beam Tension on Seismic Performance of RC Beam-Column Joints

B. L. Jiang[(1)], S. Y. Ji[(2)], Y. M. Li[(3)], Z. K. Chen[(4)], Y. Y. Tang[(5)]

[(1)] PhD Student, School of Civil Engineering, Chongqing University, jiangbaolong@cqu.edu.cn
[(2)] Associate Professor, School of Construction Management and Real Estate, Chongqing University, jishuyan@cqu.edu.cn
[(3)] Professor, School of Civil Engineering, Chongqing University, liyingmin@cqu.edu.cn
[(4)] Master Student, School of Civil Engineering, Chongqing University, czk6325165@163.com
[(5)] PhD Student, School of Civil Engineering, Chongqing University, tyyang90@126.com

Abstract

Recent studies have shown that axial tension may be experienced by beams of some structures, such as structures supported by foundations with different elevations. Thus the present study was initiated to investigate the seismic performance of interior beam-column joints under axial beam tension. This paper, by means of inelastic dynamic time history analysis, presents a comparison of seismic responses of ordinary RC frame structures and step back RC frame structures on hill slopes, showing the damage of interior beam-column joints under axial beam tension subjected to earthquake excitations. Also finite element simulation of beam-column subassemblages is investigated in this paper. By comparing the behaviors of ordinary beam-column subassemblages and beam-column subassemblages under axial beam tension subjected to lateral loads, the impact of axial beam tension on joint shear capacity is analyzed. Research results indicated the existence of significant axial beam tension in step back frame structures on hill slopes and loss of shear capacity when tension is experienced. Hence a realistic estimate of joint shear capacity is deemed crucial. Finally, suggestions for improvement in calculating joint shear strength demand are provided.

Keywords: beam-column joint; axial beam tension; joint shear capacity

1. Introduction

Beam-column joints can be critical regions in reinforced concrete (RC) moment frames subjected to severe seismic loads. Under the actions of seismic forces, large shear forces may be introduced into beam-column joints, which may cause a brittle failure in the joint core. Evidence from past earthquakes indicates that joint failure may result in structural failure. The key point of the earthquake resistant design for beam-column joints is to ensure and maintain the energy absorption capacity of plastic hinges of adjacent members, usually the beams, avoiding shear failure in the joint core. Therefore, it is of particular importance to estimate the real shear strength of beam-column joints under seismic loads.

Traditionally, design codes, including Chinese codes[1,2], fail to take axial beam tension into consideration when the joint shear capacity is estimated, because there is usually little axial force compared with shear force or moment in RC beams. However, recent studies have shown that axial tension may be experienced by beams of some structures, such as step back building structures on hill slopes. Results of seismic analysis of step back RC frame structures indicates that significant axial tensile forces may exist in RC beams under seismic actions and the effect of beam tension should not be overlooked in the design and analysis of RC structures[3,4].

The present study in this paper is to present a comparison of seismic responses of ordinary RC frame structures and step back RC frame structures, showing the performance of interior beam-column joints under axial beam tension subjected to earthquake excitations. Also finite element simulation of beam-column subassemblages is investigated in this paper. By comparing the behaviors of ordinary beam-column subassemblages and beam-column subassemblages under axial beam tension against seismic lateral forces, the impact of axial beam tension on joint shear capacity is analyzed. The findings from this research can be beneficial to a realistic estimate of joint shear strength for structural analysis, design, and assessment.

2. Performance comparison of joints under different axial beam force in structures

2.1 Modeling and analysis

2.1.1 Structural configurations and basic information

Two models, which are selected to carry out the contrastive analysis of behaviors of beam-column joints with or without axial beam tension, are chosen as shown in Fig.1. Both models are five-bay by five-bay reinforced concrete frames, having bay widths of 6 m in two directions, uniform story heights of 3.6 m. All beams and columns in frames are identical, with dimensions of 250mm×500mm and 600mm×600mm, respectively. The thickness of slabs is 100 mm. The dead and live uniform load are 4.5 kN/m^2 and 2.0 kN/m^2, respectively, and the line load applied on frame beams considering infilled wall is 12 kN/m. The main difference between these two models is that Model-1 is ordinary structure supported by foundations with equal elevation while Model-2 is step back structure supported by foundations with different elevations. In Model-2, foundations of two bays (three columns) are lifted by two floors' height (7.2 m).

Both models are designed according to *Code for design of concrete structures*[1] and *Code for seismic design of buildings*[2]. As shown in Fig.1, the two structures are symmetrical along axis Y, so typical single frames along axis X are chosen to represent structures, respectively, in the following analysis.

2.1.2 Finite element model

ABAQUS (version 6.10-1) is used to build finite element models and conduct nonlinear dynamic time history analysis. In order to analyze the local damage of beam-column subassemblages in large scale structures, structural multi-scale finite element analysis is used, which is a method that may couple the efficient coarse elements and the accurate refined elements in a model[5].

As Fig.2 shows, the concrete of Joint-J is modeled by 8-noded hexahedral (brick) elements, and the concrete damaged plasticity (CDP) model in ABAQUS is used to simulate the inelastic behavior of concrete. The concrete damaged plasticity model is primarily intended to provide a general capability for the analysis of concrete structures under cyclic and/or dynamic loading[6]. The plastic-damage model in ABAQUS is based on the models proposed by Lubliner *et al.*[7] and by Lee and Fenves[8]. According to *Abaqus/CAE User's Manual*[6], the adopted values of basic parameters of the concrete damaged plasticity model including dilation angle, eccentricity (flow potential eccentricity), fb0/fc0 (the ratio of initial equibiaxial compressive yield stress to initial uniaxial compressive yield stress), K (the ratio of the second stress invariant on the tensile meridian to that on the compressive meridian), and viscosity parameter are 30, 0.1, 1.16, 0.667 and 0.005, respectively. In the concrete damaged plasticity model, concrete behavior or damage of compression and tension are defined according to the Appendix C of *Code for design of concrete structures*[1]. The reinforcement of Joint-J is modeled as elasto-plastic truss elements, which is embedded into concrete elements to make them work together with concrete.

The other members of the frames are modeled by using a first-order 3D Timoshenko beam element (B31) with the uniaxial concrete constitutive model proposed by Scott *et al.*[9]. The steel reinforcement is defined as a smeared layer with a constant thickness equal to the area of each reinforcement bar.

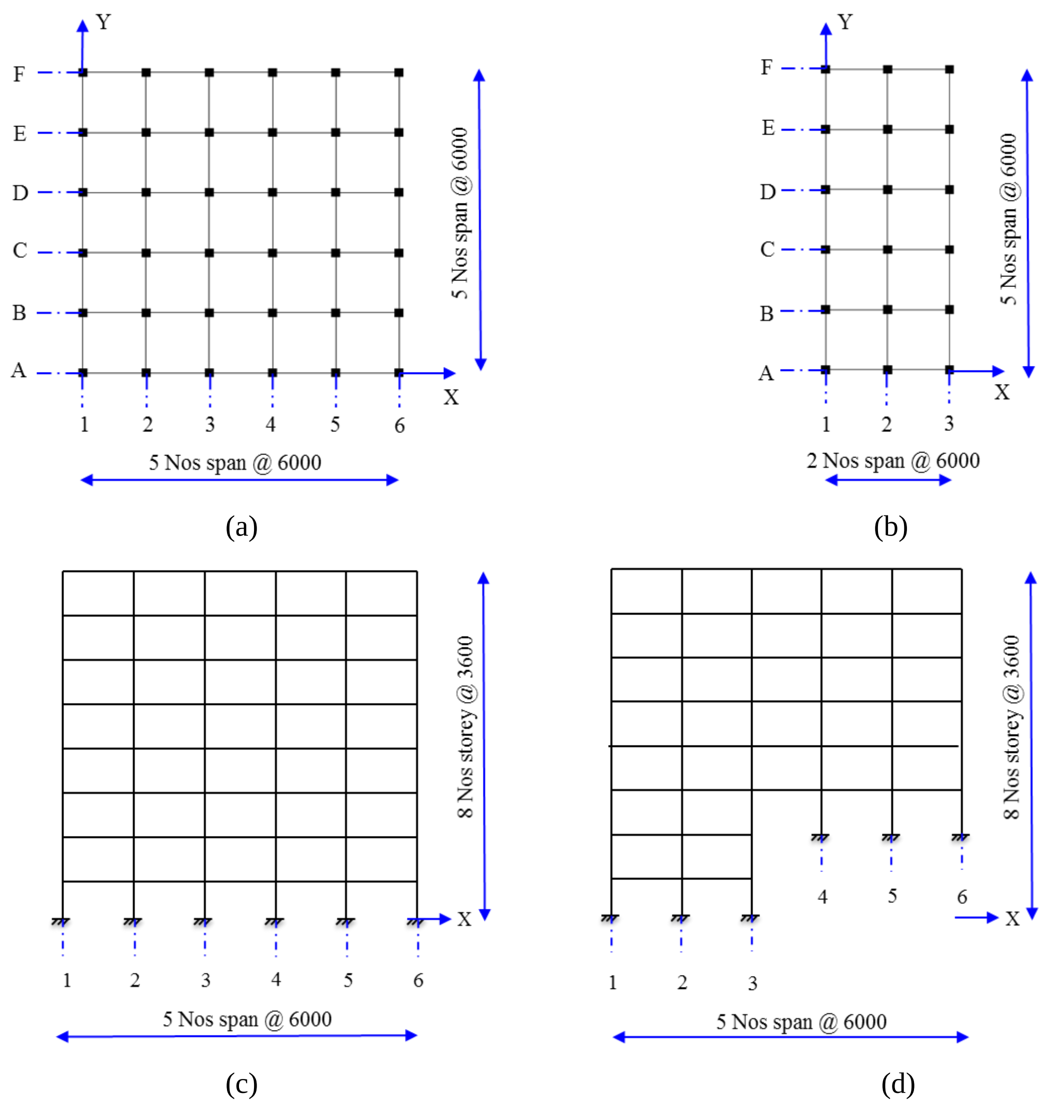

Fig. 1 – Plan and elevation of models (all dimensions are in mm): (a) floor plan of Model-1 (3rd to 8th floor plan of Model-2); (b) 1st to 2nd floor plan of Model-2; (c) elevation of Model-1; (d) elevation of Model-2.

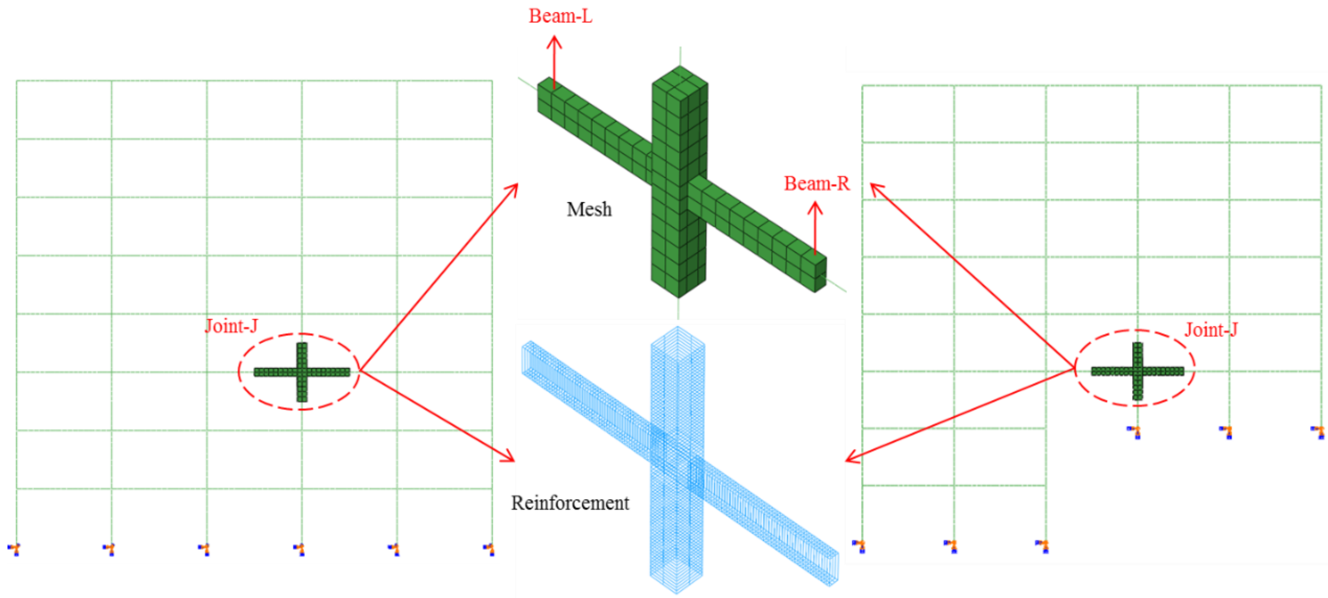

(a) (b) (c)

Fig. 2 – Finite element model: (a) Model-1; (b) mesh and reinforcement of Joint-J; (c) Model-2.

2.1.3 Material properties

The concrete strength grade selected is C30, for which the design values of compressive strength and tensile strength are 28.1 MPa and 2.8 MPa respectively, and the modulus of elasticity is 29100 MPa. Properties of reinforcement used in models are listed in Table 1.

Table 1 – Properties of the steel reinforcement

Reinforcement grade	Yield stress (MPa)	Ultimate stress (MPa)	Modulus of elasticity (MPa)
HPB300	356	498	210000
HRB400	458	618	200000

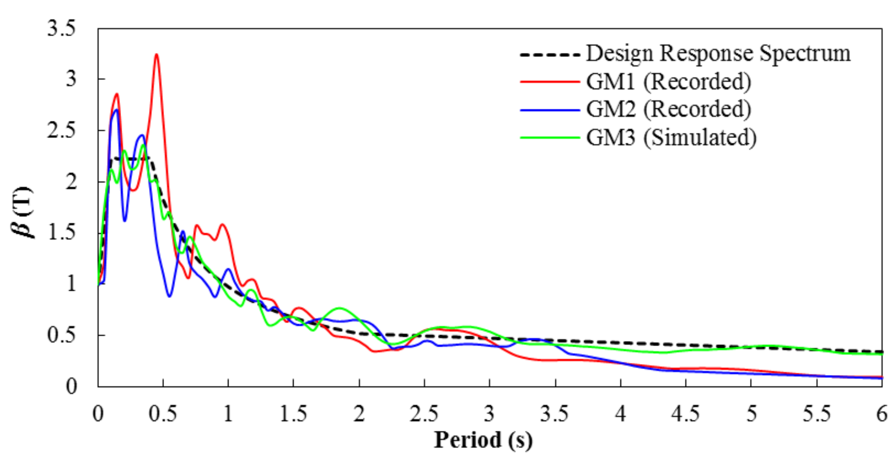

Fig. 3 – Response spectra

2.1.4 Ground motions

According to best match with the response spectrum of Chinese seismic design code[2], two recorded ground motion time histories (GM1 and GM2) and one simulated ground motion time history (GM3) are selected. In order to perform nonlinear dynamic time history analysis, all the time histories are scaled to the level of rare earthquake with a PGA of 125 cm/s^2, which means 2% probability of exceedance in 50 years. The normalized response spectra are illustrated in Fig.3 when damping ratio is 0.05.

2.2 Analytical results of time-history analysis

2.2.1 Comparison of axial beam forces

Sectional axial force time histories of Beam-L in Model-1 and Model-2 under selected ground motions are shown in Fig.4, and there are some rules.

1) There are axial forces generated in frame beams of Model-1 and Model-2 under horizontal earthquake actions. Both axial compression and tension occur in Beam-L of Model-2 due to the cycle loads, and the axial beam force appears mainly as tension in Model-2. But the main axial beam force is compression in Model-1.

2) Except the axial beam compression under GM1, other axial beam compression and tension in Model-2 are obviously larger than those in Model-1. This indicates that the axial beam force in Model-1 is on a low level (-167.828 kN to 0), while the force in Model-2 is on a high level (-314.55 kN to 428.753 kN).

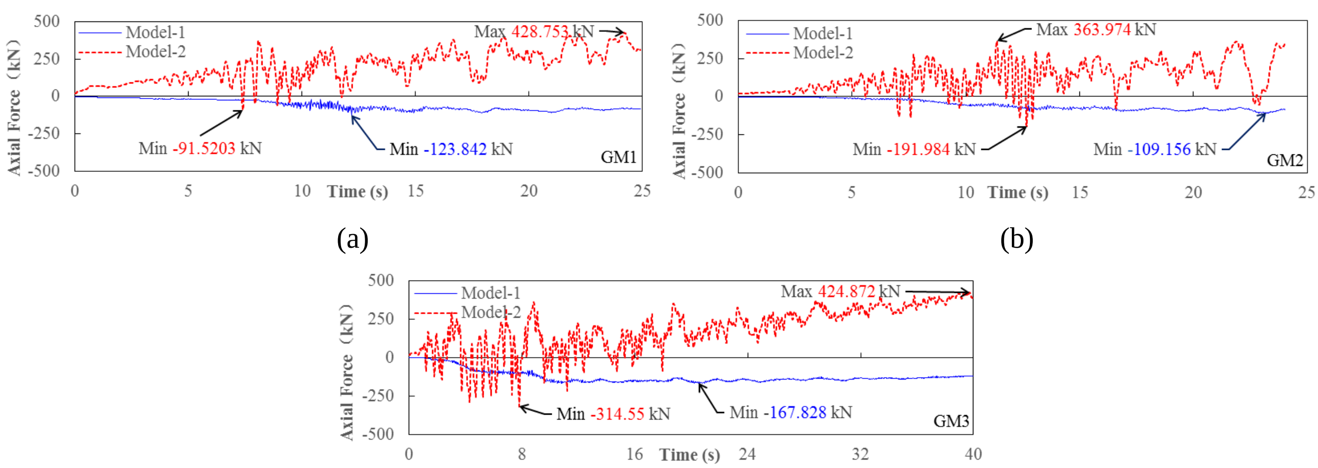

(c)

Fig. 4 – Axial force time histories of Beam-L: (a) GM1; (b) GM2; (c) GM3.

To investigate the differences of joint with or without beam axial force, Model-3 is established based on Model-2, as shown in Fig.5. The process is as follows: (1) Extract the axial force time histories of Beam-L and Beam-R of Joint-J in Model-2 under seismic ground motions; (2) Average the two axial force time histories of two sides of Joint-J under one ground motion; (3) Apply the average axial force time history to left and right side of Joint-J in opposite direction and conduct the corresponding time history analysis. Thus the axial forces of Beam-L and Beam-R can be cut down in Model-3.

As Table 2 shows, the axial forces decrease remarkably when the couple of axial force time histories are applied to Joint-J in Model-3, and the forces are close to those of beams in ordinary frame structure Model-1.

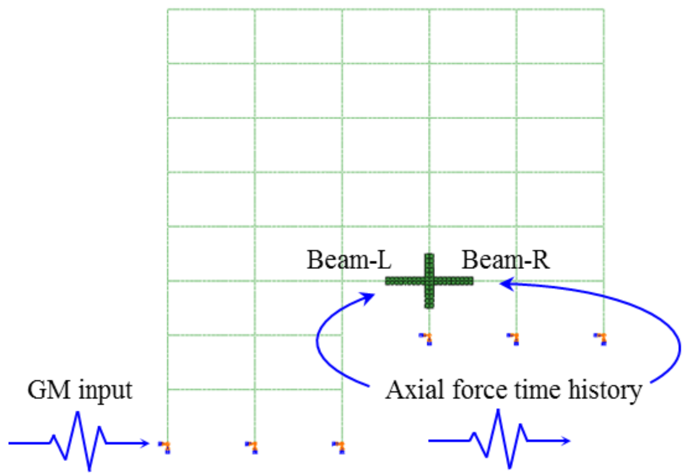

Fig. 5 – Model-3

Table 2 – Axial beam forces under seismic ground motions

Models	Beams	Type of Force	Forces (kN) GM1	GM2	GM3
Model 1	Beam-L	Max Axis Force	-1.2	-1.0	-1.1
		Min Axis Force	-124	-109	-168
		Average Axis Force	-58	-52	-124
	Beam-R	Max Axis Force	-0.3	-0.0	0.54
		Min Axis Force	-88	-85	-144
		Average Axis Force	-42	-37	-105
Model 2	Beam-L	Max Axis Force	429	364	425
		Min Axis Force	-92	-192	-315
		Average Axis Force	204	130	183
	Beam-R	Max Axis Force	185	168	183
		Min Axis Force	-78	-153	-247
		Average Axis Force	78	36	38
Model 3	Beam-L	Max Axis Force	141	145	147
		Min Axis Force	-0.1	-54	-62
		Average Axis Force	79	61	82
	Beam-R	Max Axis Force	12	42	27
		Min Axis Force	-118	-91	-107
		Average Axis Force	-42	-33	-61

2.2.2 Story drift

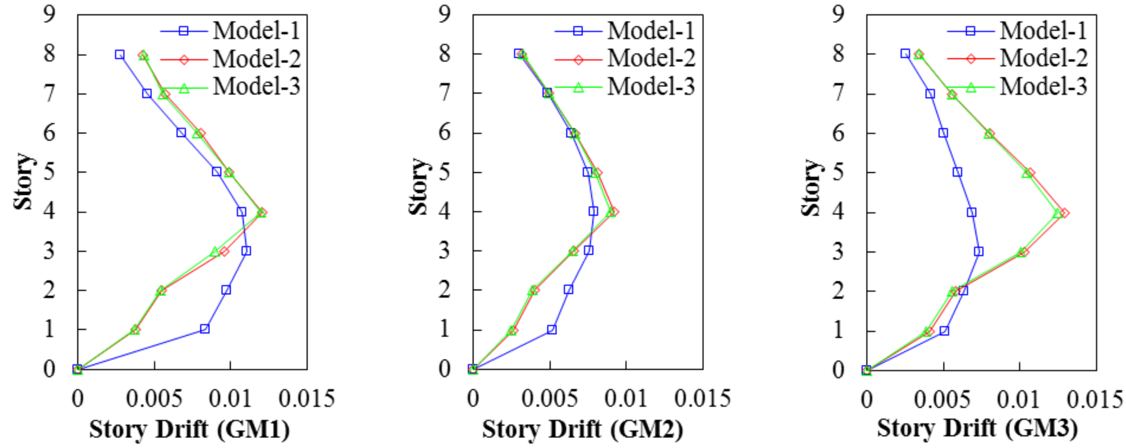

(a) (b) (c)

Fig. 6 – Story drift of models: (a) GM1; (b) GM2; (c) GM3.

Story drifts of structures are presented in Fig.6. Elasto-plastic story drifts of these three models meet the story drift limit (2%) of frame structure subjected to rare earthquake according to Chinese code[2]. Sudden change exists in the 4th story of Model-2 and Model-3. The reason for the sudden change may be attributed to the irregularity of lateral stiffness. Also, the maximum story drift of Model-2 is larger than others', just appearing in the 4th story. The large axial beam force in Model-2 may make a contribution to that.

2.2.3 Damage of joints

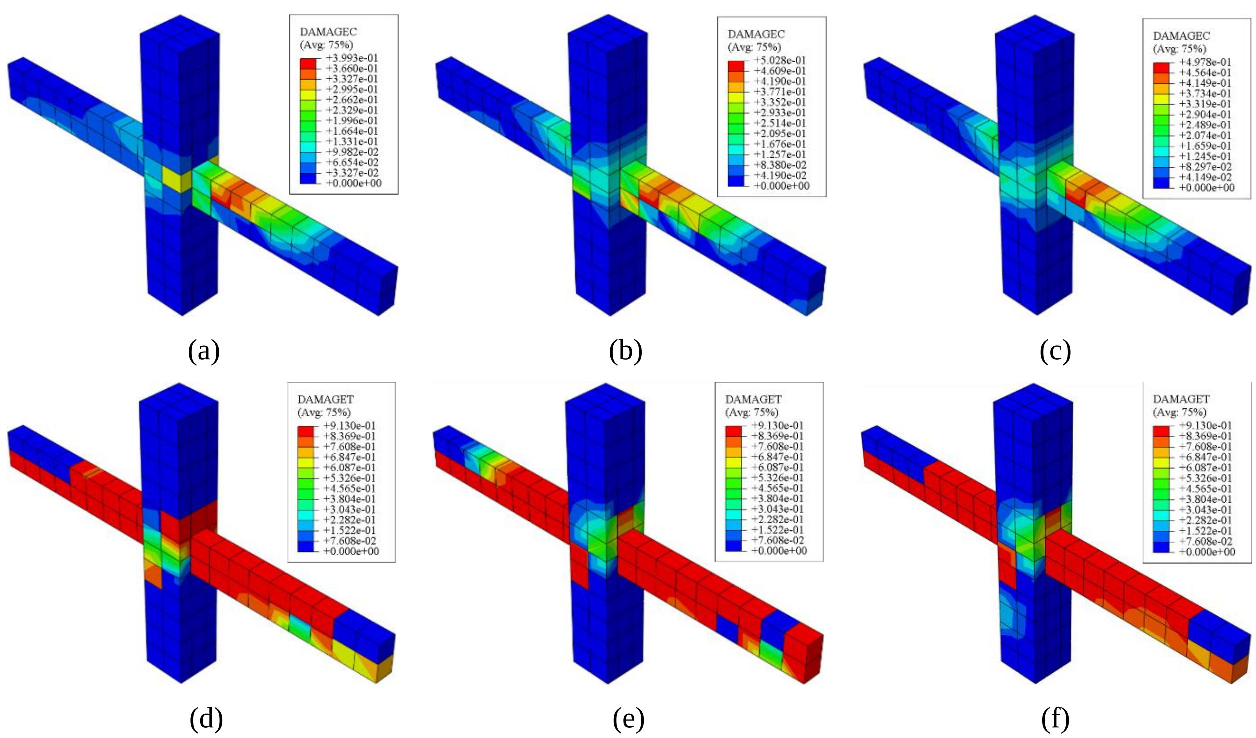

Fig. 7 – Final damage of Joint-J under GM2: (a) compression damage of Model-1; (b) compression damage of Model-2; (c) compression damage of Model-3; (d) tension damage of Model-1; (e) tension damage of Model-2; (f) tension damage of Model-3.

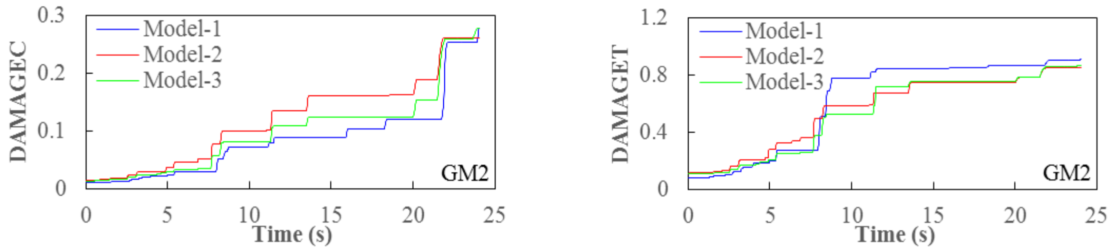

(a) (b)

Fig. 8 – Max damage time histories of joint core concrete of Joint-J under GM2: (a) compression damage; (b) tension damage.

The compression and tension damage rules of three models under three ground motions are almost same, so damage of joints under GM2 is shown in Fig.7 and Fig.8 for examples. The damage rules of three models are similar, and the damage is not symmetric with respect to joint due to asymmetric loads or structure. By comparison, the damage of Model-2 is more serious than that of Model-3, which may result from larger axial beam tension in Model-2.

3. Finite element analysis of joints under different axial beam force

For further study on the influence of axial beam tension on capacity of beam-column joints, five finite element models of beam-column subassemblages with variations in axial beam force are analyzed.

3.1 Finite element modelling

Finite element models of beam-column subassemblages are built according to Joint-J in Section 2. The element types and material properties are also all the same as Joint-J. The modelling information is shown in Fig.9.

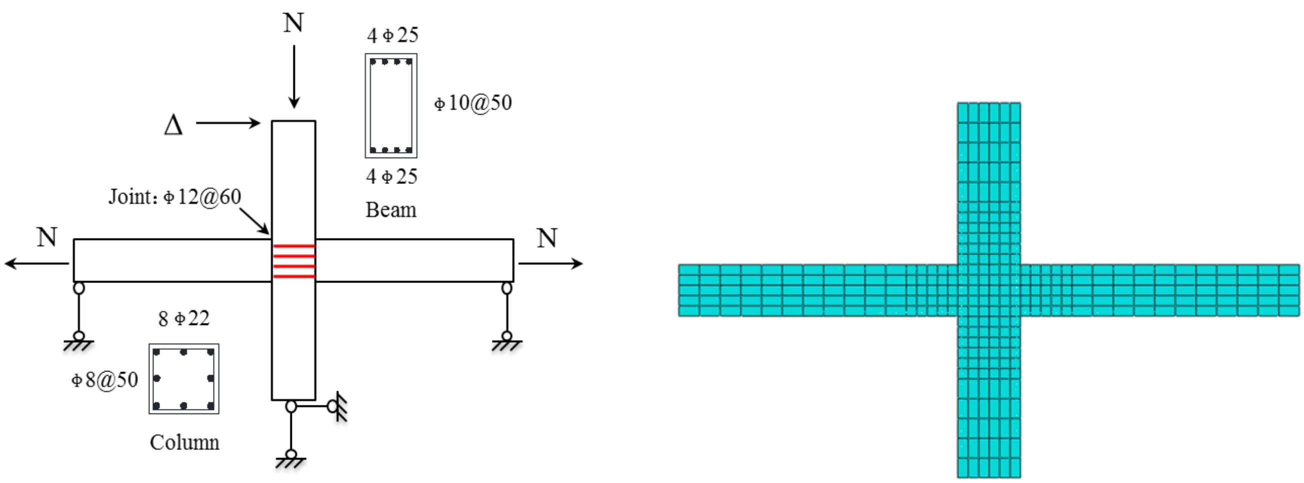

(a) (b)

Fig. 9 – Information of models: (a) schematic drawing; (b) finite element mesh.

3.2 Applying loads

In the analysis of five models, axial loads on columns remain constant with a axial force ratio of -0.3 (n=-0.3). Here, the meaning of n is axial force ratio. The value of n is equal to $N/(f_{c*}A)$ when N < 0. Nevertheless, The value of n is equal to $N/(f_{y*}A_s)$ when $N > 0$. N denotes the axial force, and the value is negative when axial compression occurs, otherwise, the value is positive. f_c and f_y denote the design value of axial compressive strength of concrete and tensile strength of reinforcement respectively. A and A_s denote the total area of concrete section and total sectional area of longitudinal bar respectively.

The axial beam force ratios of the five models are n=-0.2, -0.1, 0, 0.1 and 0.2, respectively. Axial loads of beams also remain constant during analyzing.

In this study, the general static analysis method is employed. Displacement control is applied. Loading is enforced displacement applied to the top of the column as shown in Fig.9. The applied displacement is linearly increased from 0 to a drift of 2%.

3.3 Results and discussions

3.3.1 Stress and damage

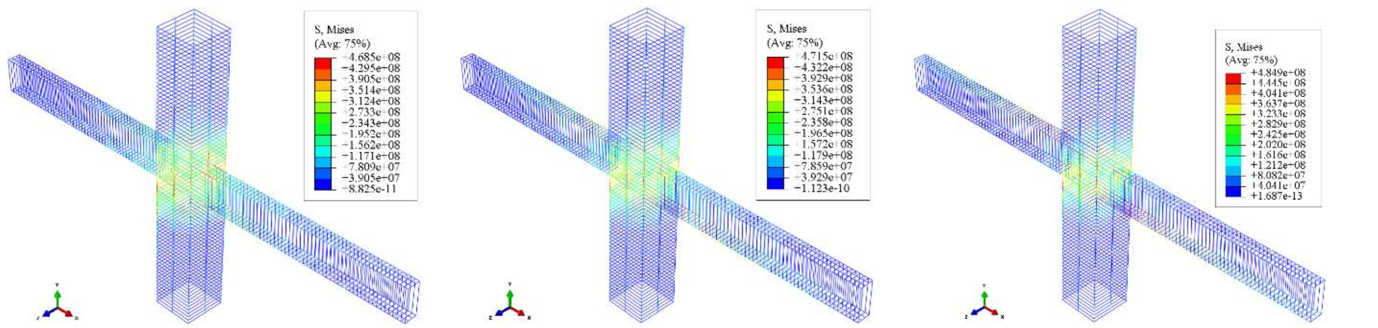

(a) (b) (c)

Fig. 10 – Mises Stress of reinforcement: (a) n = -0.2; (b) n = 0; (c) n = 0.2.

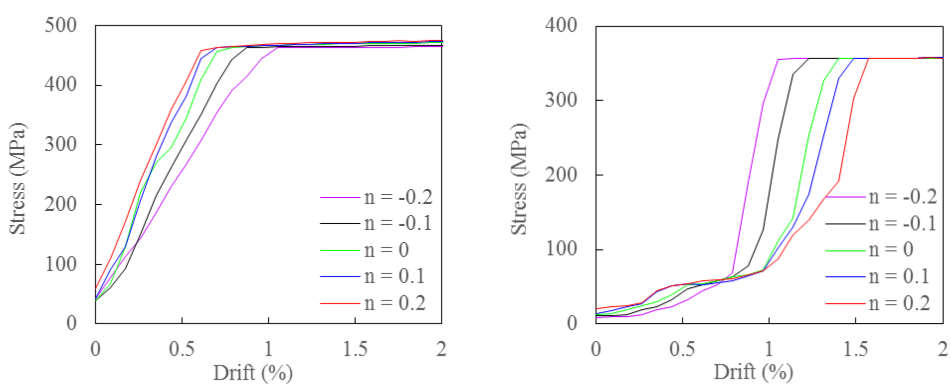

(a) (b)

Fig. 11 – Mises Stress of reinforcement: (a) joint hoops; (b) beam longitudinal reinforcement.

As presented in Fig.10 and Fig.11, the yield of reinforcement mainly appears in joint core zones and ends of adjacent beams. As shown in Fig.11, the stress of longitudinal bars in beams and stirrups in joints reached the yield strength before failure of beam-column connections. Longitudinal bars in beams have already yielded before the yield of the stirrups in joints. More importantly, with the axial beam force varying from compression to tension (n ranging from -0.2 to 0.2), longitudinal bars in beams yield earlier and earlier, while the stirrups in joints yield correspondingly later and later.

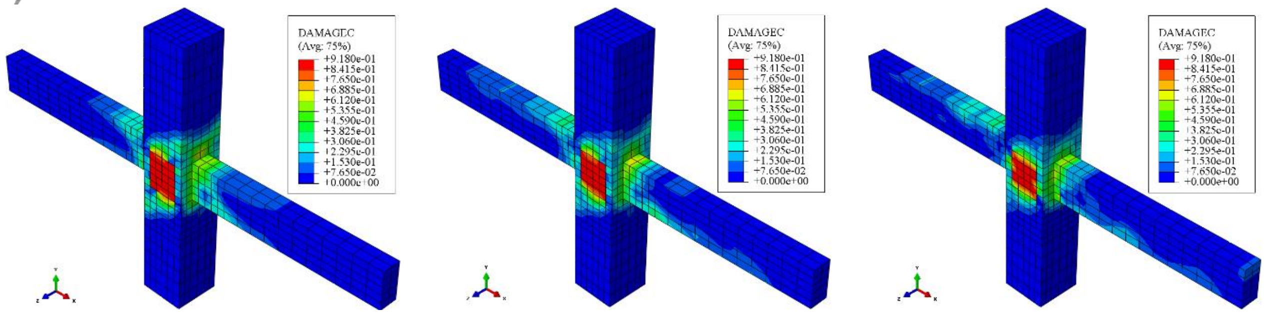

(a) (b) (c)

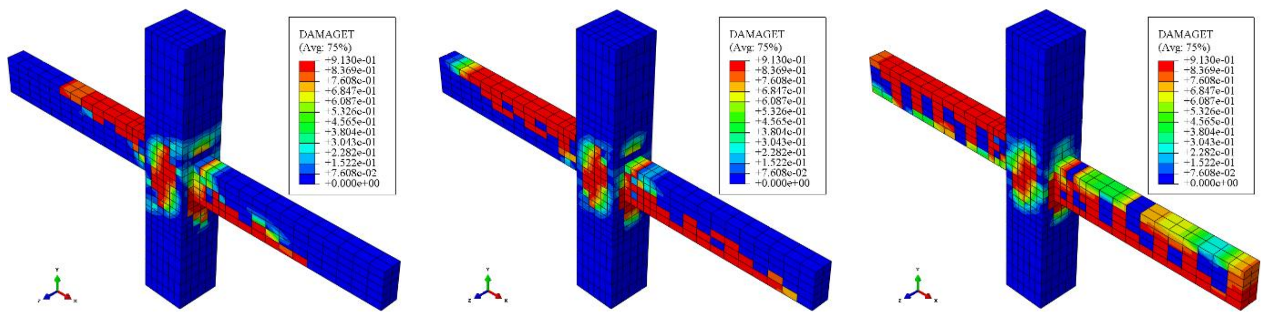

(d) (e) (f)

Fig. 12 – Final damage of joint models: (a) n = -0.2, compression damage; (b) n = 0, compression damage 2; (c) n = 0.2, compression damage of Model-3; (d) n = -0.2, tension damage; (e) n = 0, tension damage; (f) n = 0.2, tension damage.

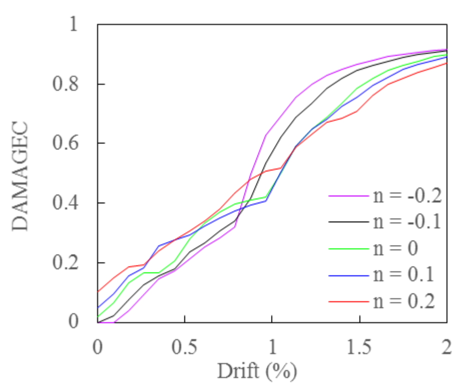

(a)

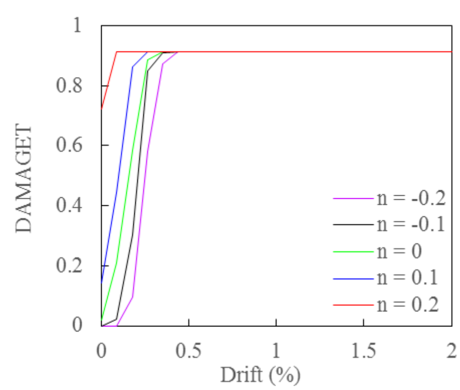

(b)

Fig. 13 – Max damage of joint core concrete: (a) compression damage; (b) tension damage.

As shown in Fig.12, the damage of joint models is mainly concentrated in joint core zones and plastic hinge regions of adjacent beams. It can be inferred that the beam damage of compression and tension results from flexural stress and tensile stress in both ends of beams, and the joint damage results from the diagonal compression strut of joint concrete. Thus with the axial force ratio n ranging from -0.2 to 0.2, the damage regions of compression and tension become larger and larger. The Fig.13 depicts the relationship between the max damage of joint core concrete and the drift. The initial compression or tension damage indices of the five models differ from each other due to the combinations of initial axial forces applied on columns and beams. Furthermore, with n ranging from -0.2 to 0.2, the tension damage develops more and more rapidly, which is contrary to the compression damage. Finally, the larger axial beam compression leads to the greater compression damage.

The damage of concrete and stress of reinforcement above in Fig.10~Fig.13 indicates that the failure mode of all these five joint models is a pure joint shear-failure mechanism referring to joint failure after plastic hinges develop at both ends of adjacent beams.

3.3.2 Ultimate strength

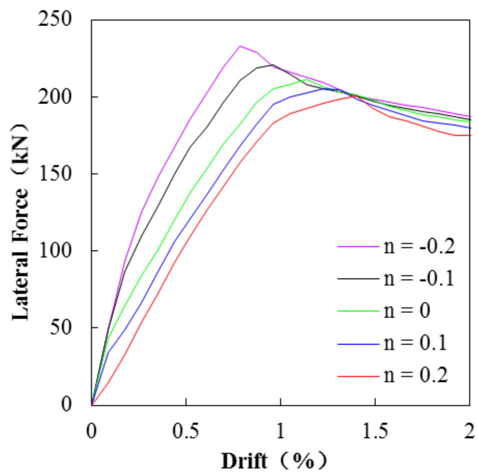

Fig. 14 – Lateral load-drift curves of joint models

Table 3 – Ultimate loads of joint models

Axial beam force ratio *n*	-0.2	-0.1	0.0	0.1	0.2
Ultimate lateral load (kN)	233	221	211	205	201
Joint shear capacity (kN)	1664	1581	1509	1473	1437

An accurate estimate of the shear capacity of joint zone could only be obtained when the pure shear failure is ensured. Since, as mentioned previously, the failure mode of all the models is the pure shear failure, the joint shear capacities are obtained in Tabale 3. With n ranging from -0.2 to 0.2, the joint shear capacity reduces from 1164 kN to 1437 kN. Especially when n equals 0.1 and 0.2 with tensions in beams, the joint shear capacity decreases 2.4% and 4.8% respectively compared with n = 0. Also, similar rules of ultimate lateral loads are presented in Tabale 3 and Fig.14.

According to finite element analysis results, axial beam tension weakens shear capacity of beam-column joint, and the larger axial tension appears in beam, the more decrease of shear capacity happens. The reason may be that the concrete contribution to the shear resistance of the joint is hampered by the axial beam tension. Consequently, the confinement of core concrete is inefficient in joint zones subjected to tensile stresses when the development of axial tension takes place in beams. In this situation, lateral joint reinforcement need to be improved.

4. Conclusions

This paper presents nonlinear dynamic time history analysis and finite element analysis to study on influence of axial beam tension on seismic performance of beam-column joints. From the analytical results, the following conclusions can be drawn:

1) Beams in such complex structures as step back building structures on hill slopes may experience remarkable axial forces, especially tensions, under horizontal earthquake excitations. Moreover, the axial forces are usually much larger than those of beams in ordinary structures.

2) According to finite element analysis conducted, the seismic behavior of a beam-column joint is sensitive to axial beam force variation. The increase in axial beam tension, as well as the decrease in axial beam compression, will result in reductions of the joint shear capacity. In this case, joint shear strength becomes lower with the larger axial beam tension.

3) When beams are likely to experience axial tensions, RC beam-column joints should be designed with the consideration of the shear capacity reduction resulting from influence of axial beam tension. Thus strength capacities of beam-column joints will be more accurately evaluated and assessed, providing a safer structure.

5. Acknowledgements

The research in this paper was supported by the National Natural Science Foundation of China (51638002, 51478067 and 51478068).

6. References

[1] Ministry of Housing and Urban-Rural Development of the People's Republic of China (2010): *Code for design of concrete structures (GB 50010-2010)*. China Architecture & Building Press, Beijing, China.

[2] Ministry of Housing and Urban-Rural Development of the People's Republic of China (2010): *Code for seismic design of buildings (GB 50011-2010)*. China Architecture & Building Press, Beijing, China.

[3] Huang LJ (2014): Study on Seismic Design Measures of RC Frame Cliff-Structures. Master's thesis, Chongqing University, Chongqing, China. (in Chinese)

[4] Li L (2015): Study on Tensile Characteristics of Beams in RC Frame Structures Supported by Foundations at Different Ground Levels. Master's thesis, Chongqing University, Chongqing, China. (in Chinese)

[5] Lu XZ, Lin XC, Ye LP (2008): Multiscale Finite Element Modeling and its Application in Structural Analysis. *Journal of Huazhong University of Science and Technology (Urban Science Edition)*, **25** (4), 76-80. (in Chinese)

[6] Dassault Systèmes (2010): *Abaqus/CAE User's Manual (version 6.10)*. Dassault Systèmes Simulia Corp., Providence, RI, USA.

[7] Lubliner J, Oliver J, Oller S, Oñate E (1989): A plastic-damage model for concrete. *International Journal of Solids and Structures*, **25** (3), 299-326.

[8] Lee J, Fenves GL (1998): Plastic-damage model for cyclic loading of concrete structure. *Journal of Engineering Mechanics*, **124** (8), 892-900.

[9] Scott BD, Park R, Priestley MJN (1982): Stress-Strain Behavior of Concrete Confined by Overlapping Hoops at Low and High Strain Rates. *Journal of the American Concrete Institute*, **79** (1), 13-27.